Adsorption and Solvation of HCl into Ice Surfaces

S. Haq, J. Harnett, and A. Hodgson*

Surface Science Research Centre, The University of Liverpool, Liverpool L69 3BX, U.K.

Received: October 25, 2001; In Final Form: January 17, 2002

The kinetics of HCl adsorption and incorporation into crystalline and amorphous ice were studied by using a thermal molecular beam, with FTIR spectroscopy to characterize the products. Thin films of hexagonal ice were grown on Pt(111) to provide a highly ordered surface on which to test models for HCl adsorption. Absolute HCl uptakes, product H_2O:HCl stoichiometries, and sticking probabilities were measured as a function of HCl exposure and temperature between 85 and 145 K. Adsorption proceeds via a trapping mechanism, with the barrier to HCl adsorption into the final state being 7 kJ mol^{-1} lower than for desorption at low coverages. Adsorption becomes less favorable with increasing HCl coverage, saturating with one HCl adsorbed for each surface H_2O molecule, independent of the ice thickness for $T \leq 120$ K. Above 125 K, HCl is incorporated into the ice film, absorption showing a complex exposure and flux dependence. HCl absorption disrupts the ice lattice, causing the rate of HCl uptake to increase as adsorption proceeds. At high HCl fluxes, the creation of favorable adsorption sites on the ice surface is limited by the rate of HCl transport into the film and the sticking probability drops. The saturation product for $130 \leq T \leq 140$ K is the amorphous trihydrate $HCl\cdot(3.1 \pm 0.3)H_2O$ and RAIR spectra for this, and for the surface-adsorbed monohydrate species, showed no bands due to molecular HCl. Amorphous ice films show a similar behavior, but with a greater density of water in the surface and more facile HCl transport into the film.

1. Introduction

Heterogeneous reactions in the polar stratosphere play an important role in converting chlorine-containing species from relatively stable reservoir compounds such as HCl and $ClONO_2$ into active chlorine. The polar stratospheric clouds (PSC's) responsible for this chemistry are composed of either nitric acid/ice mixtures or pure water ice particles, the latter forming at approximately 187 K in the relatively dry atmosphere. The heterogeneous reaction between HCl and $ClONO_2$ on these PSC's is an important source of chlorine in the polar vortex during the winter months, the chlorine being photolyzed when spring returns and initiating the dramatic loss of ozone. The reaction is believed to go via direct reaction between $ClONO_2$ and HCl, which is preadsorbed on the ice surface,

$$ClONO_2(g) + HCl(s) \rightarrow Cl_2(g) + HNO_3(s)$$

For this reaction to produce chlorine efficiently, HCl must be readily adsorbed and available for reaction on the PSC surfaces.

Because of its critical role, the adsorption and reaction of HCl molecules on water and acid ice surfaces has been investigated extensively. At temperatures characteristic of the stratosphere, water is labile, with rapid adsorption and desorption from the surface. This complicates studying the reactivity of HCl on these surfaces, adsorption and diffusion being difficult to separate from processes which lead to burying of the adsorbate under deposited water. Experimental measurements under temperature and water vapor pressure conditions appropriate to the atmosphere,[1−3] for example, in flow systems,[4,5] provide kinetic measurements of uptake and reaction rates as input for modeling. However, while these experiments provide information about gas-phase products and effective reaction rates which can be extrapolated to PSC surfaces, they can give only indirect evidence about the mechanism for reaction. This has been addressed by investigating adsorption at lower temperatures[6−13] and by theoretical studies of HCl adsorption.[14−20] These studies have raised several issues about which there is conflicting evidence, notably the degree of ionization of HCl adsorbed on an ice surface, the role of defects in promoting ionization, and the stoichiometry of the hydrates formed.

IR measurements of HCl adsorption on ice have identified a molecular adsorption state at low temperature, $T < 50$ K,[7] consistent with the presence of a bound molecular state on the ice surface.[17] Molecular beam scattering studies show that energy transfer is efficient, HCl trapping at the ice surface with a high probability.[10,21,22] At higher temperatures the HCl ionized to form what was thought to be an amorphous 1:1 hydrate on the surface.[7] Banham et al.[11] confirmed the absence of molecular HCl on the ice surface above 80 K and concluded that HCl was ionized at 140 K. The broad nature of the IR spectra from amorphous films, and uncertainties in assigning the hydrate spectra,[6,7,11] lead to problems in positively identifying the products, but adsorption at 140 K was believed to form the hexahydrate,[9,11] although a recent laser desorption study suggests that the product is the trihydrate under these conditions.[23] Recently Devlin and co-workers have suggested that molecular HCl is stable on the ice surface at submonolayer coverages even at 125 K, again on the basis of IR spectra.[13]

Graham and Roberts[9] looked at the importance of the ice structure on the adsorption of HCl by comparing adsorption on amorphous and crystalline ice. They found a lower sticking probability on the crystalline ice and attributed this to preferential reaction at defect sites. The idea that HCl requires a defect site in order to dissociate and ionize seems to be inconsistent with the results of uptake experiments on thin films[11,12] while Isakson and Sitz[21] concluded that the ice phase made no

* E-mail: ahodgson@liv.ac.uk FAX +44 151 708 0662.

10.1021/jp013944z CCC: $22.00
Published on Web 03/22/2002

difference to the HCl scattering behavior. A recent study of HCl adsorption on thick (200−1000 ML) ice films did find that films grown under conditions expected to produce different morphologies showed very different HCl uptake kinetics.[24] HCl migrated into the ice film even at 100 K, a result which is surprising in view of other reports which found that HCl adsorption rapidly saturated at this temperature[10] and may be associated with transport along defects in the ice film.

There is some disagreement among the theoretical studies as to the barrier for hydration and ionization of HCl. Clary and co-workers found that HCl was weakly adsorbed onto ice clusters[15,25,26] but concluded that defects enhanced the lifetime of HCl physisorbed on ice and suggested that these sites might also enhance dissociation and ionization to form the hydrated products.[27] The degree of hydrogen bonding in the coordinating water network appears to be important in determining the barrier to HCl ionization.[26] Gertner and Hynes found that HCl would not ionize when adsorbed on the surface but does so when incorporated into a growing ice film.[16,28] Such a mechanism may help to explain how HCl adsorbs under stratospheric conditions but will not be available under low-temperature conditions where the ice surface is not labile. Casassa[18] has suggested that HCl may be able to displace water from the surface and subsequently ionize once incorporated into the ice. Recent studies of HCl adsorption on an ice Ih surface have suggested that ionization may be nonactivated when HCl is bound at favorable sites.[19,20] This study found that HCl bound molecularly on the surface but could ionize when adsorbed in a surface site which had one free O atom and two dangling H atoms to which the chlorine could bind.

In this paper we describe molecular beam measurements which establish the absolute uptake of HCl onto thin films of amorphous and crystalline ice Ih as a function of temperature and coverage in the range 85 to 140 K. We show that below 120 K HCl adsorption saturates at a coverage of 1.1×10^{15} molecules cm^{-2}, with formation of a surface containing one HCl molecule adsorbed for each water molecule originally in the surface layer. Adsorption occurs via a precursor adsorption mechanism, the barrier to adsorption being ca. 7 kJ mol^{-1} lower than for desorption from the clean ice surface, the difference falling as the HCl coverage increases toward saturation. Above 125 K, HCl begins to be absorbed into the ice film and uptake saturates with formation of HCl trihydrate. Transport into crystalline ice is self-catalyzed, HCl absorption disrupting the ice structure and increasing the transport rate. HCl adsorbs reversibly onto the trihydrate surface to form a higher hydrate, probably the same "surface monohydrate" as formed on an ice surface, the additional HCl desorbing above 130 K. The ice morphology has no effect on the HCl sticking probability but does influence the uptake of HCl onto the surface and the rate of incorporation into the film. IR spectra and temperature programmed desorption spectra of the HCl hydrate films are compared with existing reports and the mechanism for HCl adsorption is discussed.

2. Experimental Section

Adsorption of HCl was studied with a room temperature, thermal molecular beam to dose HCl on to thin layers of ice (1−150 monolayers, where 1 monolayer = 1.1×10^{15} cm^{-2}). The ice layers were grown on a Pt(111), single-crystal substrate, which was cleaned by the usual techniques of sputtering and annealing and checked for cleanliness by LEED and thermal desorption spectroscopy. The crystal was mounted on two Ta heating wires, attached to a liquid nitrogen cooled manipulator. This allowed ice films to be grown at a selected temperature ($T \geq 85$ K) or the crystal heated to desorb the film during temperature programmed desorption (TPD). Ice layers were formed by using a collimated molecular beam to deposit H_2O onto the substrate at a controlled rate, typically 0.01 ML s^{-1}. Depending on the deposition rate and temperature, crystalline hexagonal ice Ih or amorphous solid water (ASW) were formed.[29−34] Crystalline ice can also be formed by annealing ASW films close to the water desorption temperature.[35] HCl adsorption was insensitive to the substrate chosen (Pt(111), Au(111)and Pd(110) gave similar results) or to details of how the crystalline ice film was prepared. Minor differences were seen for adsorption on ASW prepared under different conditions and these can be attributed to the surface area and porosity of the ASW film.[36] All of the data described here are for H_2O films grown on a Pt(111) substrate, since this provided a well-ordered ice surface with the hexagonal R30° LEED pattern characteristic of an ice Ih film.[37−39]

The beam source used to deposit H_2O and HCl was a glass capillary, operated in the molecular flow regime with a backing pressure of a few Torr. The beam was differentially pumped by two turbomolecular pumps and defined by a skimmer and collimating tube to provide a spot 5 mm diameter on the sample. The beam intensity was calibrated by measuring the flow rate of gas through the nozzle and relating this to the partial pressure of the beam in the chamber. The relative flux of different species was found to be proportional to the backing pressure and varied with $m^{-1/2}$, as expected for an effusive beam from kinetic theory. Temperature programmed desorption (TPD) was used to characterize the ice and HCl hydrate films produced by monitoring the desorption products using a VG SX200 quadrupole mass spectrometer (QMS). Water TPD from Pt(111) shows a well-defined desorption peak for the first bilayer of water, which is separate from the multilayer peak. In combination with sticking measurements, this allowed the flux of water from the molecular beam to be calibrated accurately. RAIR spectra of the water/ice and HCl/ice layers were measured on a Mattson 6020 FTIR spectrometer with 4 cm^{-1} resolution.

Sticking probabilities, *S*, were measured for water and HCl adsorption by using the direct reflection technique of King and Wells.[40] A flag in the main chamber was used to prevent the beam from hitting the surface until desired. The partial pressure of the adsorbing gas in the main chamber was measured by using the QMS and the fraction of the incident molecular beam which adsorbs on the surface was determined from the decrease in the partial pressure as the beam was allowed to strike the surface. This technique measures the net removal of HCl by the surface, it does not reflect temporary adsorption of HCl such as may occur during trapping into a weakly bound state which desorbs rapidly and reversibly on a time scale of less than ~1 s. Since physisorbed HCl desorbs near 50 K,[8,9] this state is not observed directly and the sticking probabilities *S* measured here reflect the probability of HCl hydrating and becoming adsorbed irreversibly at the ice surface. In contrast the term "trapping" will be used to describe temporary adsorption into a weakly bound state, such as the physisorption state, from which it may desorb freely at the temperature of these experiments ($T \geq 85$ K). The net sticking probability *S* is obtained with an accuracy of ca. ±0.02 and a similar lower limit on the values of *S* which can be measured. The coverage dependence $S(\Theta)$ was determined from the time behavior of the HCl uptake traces. These were converted to an absolute scale by using TPD to establish the total uptake on the surface. The absolute coverage of water was easily determined by using the characteristic TPD profile

for the first bilayer of water on Pt(111), and the uptake of HCl was calibrated relative to this, using the relative beam fluxes of H_2O and HCl. HCl coverages are quoted in monolayers, referenced to the water density in the ideal hexagonal R30° overlayer on Pt(111).

3. Results and Discussion

A. Growth of Ice Films on Pt(111). Thin ice films were grown by choosing the surface temperature, beam flux, and exposure appropriately to terminate adsorption of H_2O after the first bilayer or to grow a crystalline ice film with a precisely controlled thickness. Water adsorption onto the Pt(111) surface at a temperature above 135 K produces a stable bilayer of crystalline hexagonal ice.[33,38] TPD profiles show a peak at 170 K due to desorption of the first bilayer, with a multilayer desorption peak at ~160 K forming for higher exposures. The first water bilayer shows a $(\sqrt{39} \times \sqrt{39})$R16.1° LEED pattern, consistent with a recent He atom scattering study of H_2O adsorption on this surface,[33] but this changes to a hexagonal R30° structure as H_2O multilayers condense.[39] The most highly ordered films were obtained by growing ice films slowly (0.01 ML s^{-1}) at a temperature of 135 K or above where water molecules are mobile on the surface. These films showed sharp LEED patterns, indicating the formation of an ordered ice film whose quality is probably limited only by the step density of the original metal surface.[41] FTIR spectra for crystalline H_2O ice layers showed three sharp peaks at 3360, 3258, and 3154 cm^{-1}, compared to the broad single peak which is found for amorphous solid water (ASW) formed by adsorption at 90 K, Figure 1a. Crystalline ice could also be formed by annealing an ASW film close to the water desorption temperature. Films formed in this way showed crystalline RAIR spectra and displayed identical behavior toward HCl adsorption.

Water adsorption at 90 K results in the formation of a disordered, amorphous solid water film, with a diffuse LEED pattern. At this temperature the mobility of H_2O on the surface is negligible and the water molecules are adsorbed at the site where they initially trap. An amorphous ice film develops which has a substantially reduced degree of hydrogen-bonding but is expected to be relatively dense, given the normal incidence of the incident H_2O beam.[36] ASW shows up in the FTIR spectra as a broad peak at 3392 cm^{-1}, with a weak but sharp band at 3695 cm^{-1} which has been attributed to free OH groups on the ice surface.[42]

B. HCl Adsorption on Ice at 90 K. Adsorption of HCl on crystalline ice at 90 K results in the uptake profile shown in Figure 2. The initial sticking probability of HCl is large, $S_0 = 0.97 \pm 0.02$, and adsorption remains extremely efficient until the surface saturates with HCl. The absolute uptake of HCl was determined by calibrating the flux of HCl in the beam relative to the H_2O flux required to form a single bilayer of ice on the surface. The saturation uptake of HCl was determined to be 1.0 ± 0.1 monolayer at 90 K for crystalline ice Ih, corresponding to a saturation surface coverage of 1 HCl for each water molecule originally adsorbed in the surface layer. This ratio is insensitive to the thickness of the water ice layer, indicating that HCl is adsorbed only onto the surface and does not incorporate into the film. This is in contrast with recent adsorption measurements on thicker ice films where HCl was reported to incorporate into the ice film even at 100 K, possibly by migration along grain boundaries.[24] For thick ice films we find the HCl uptake increases slightly, probably associated with a roughening and an increase in the surface area of these films.

When HCl adsorption is repeated on amorphous solid water ice, the uptake profile is similar (Figure 2) but saturates with ca. 50% more HCl adsorbed. The initial sticking probability is the same as for crystalline ice to within our experimental error (±2%). Nitrogen uptake measurements by Kay and co-workers[43] have shown that even a dense, nonporous ASW film still has a 40% higher surface area than that for crystalline ice, presumably caused by surface roughness. Adsorption on ASW is consistent

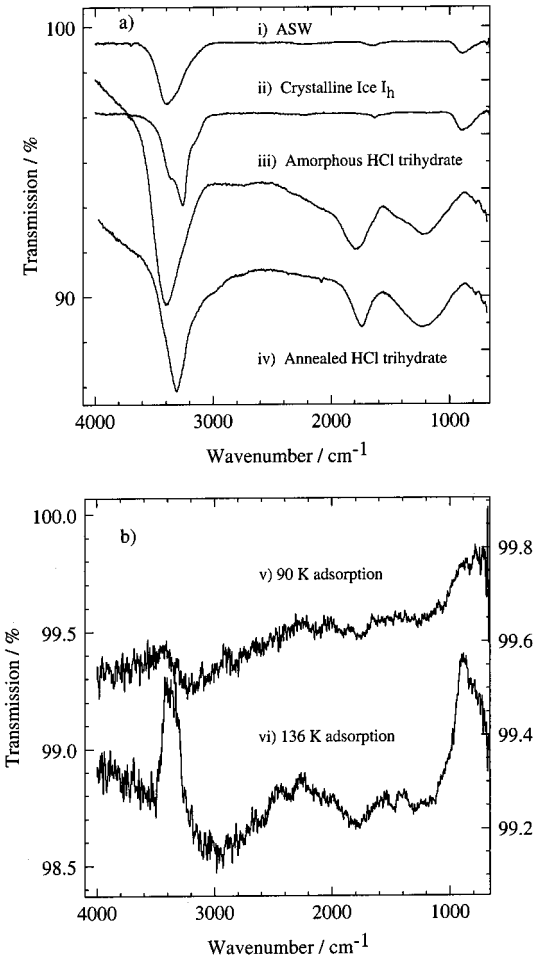

Figure 1. (a) RAIR spectra for crystalline and amorphous ice and HCl trihydrate layers: (i) ASW, (ii) crystalline ice Ih, (iii) amorphous HCl trihydrate formed by exposing a 70 ML film of water to a beam of HCl, (iv) the same film after annealing to 170 K during TPD. (b) Difference spectra showing the change in the RAIR signal upon HCl adsorption for (v) monolayer adsorption at 90 K and (vi) during adsorption to form bulk amorphous HCl trihydrate at 136 K.

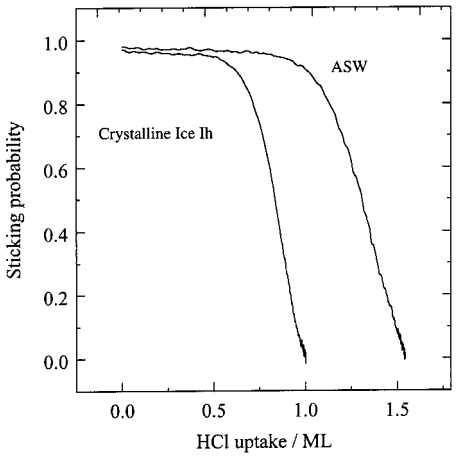

Figure 2. Adsorption of HCl on crystalline ice and amorphous solid water at 90 K as a function of coverage.

with a similar increase in the density of final adsorption sites for HCl on the ASW surface and rules out a difference in sticking probability. This finding is in contrast with the conclusions of Graham and Roberts,[9] who reported that the adsorption probability on crystalline ice was 60% of that on amorphous solid water surfaces at 120 K based on uptake versus exposure measurements. They attributed this difference to an increased adsorption probability at steps or defects in the ice surface, whereas we see no significant change in S (Figure 2). The discrepancy is probably due to the limited precision of the uptake versus exposure measurements[9] which were unable to distinguish a change in sticking probability from a change in surface area of the ice film.

The sticking coefficient of HCl remains almost constant, independent of surface coverage, until adsorption is nearly complete, Figure 2. This slow decrease in $S(\Theta)$ with coverage is characteristic of a precursor-trapping mechanism where HCl is initially adsorbed into a weakly bound precursor state.[44,45] Since the adsorption rate does not decrease with coverage, this state must be available on both bare and HCl-covered ice as an extrinsic precursor. HCl trapped in the precursor state is sufficiently mobile to diffuse to a favorable binding site, dissociation competing efficiently with desorption back to the gas phase to maintain a constant adsorption rate as the HCl coverage increases. The precursor is probably the molecular physisorption state,[17] which is typically relatively insensitive to the orientation or site of adsorption. Subsequent desorption or transfer into the final adsorption state can be described by kinetic models which describe partitioning between desorption and adsorption into the stable well from the precursor state.[44,45] This leads to an adsorption probability which depends on temperature, determined by the relative barrier for these two channels.

There is already some evidence in the literature for the presence of a molecular HCl precursor state on water ice. Devlin and co-workers[7] have reported IR bands characteristic of molecular HCl adsorbed on ice at temperatures below 50 K, consistent with calculations which estimate a physisorption well depth of ca. 35 kJ mol^{-1} on ice Ih.[17] Above 60 K molecular HCl was converted to an amorphous hydrate, which was partially ionized and had an IR spectrum that resembled that of the amorphous 1:1 hydrate. This behavior is consistent with HCl trapping into a metastable molecular state at low temperatures and transferring into a more tightly bound, hydrated state as the temperature increases. Even at much higher temperatures a high partial pressure of HCl results in the formation of physisorbed HCl layers on top of the HCl hydrate, with characteristic RAIR bands between 2706 and 2764 cm^{-1}.[11] Difference spectra for adsorption of a single monolayer of HCl on ASW at 85 K (Figure 1b,v) are dominated by loss of intensity from the water bands but also show weak, broad adsorption bands near 1750, 2150, and 3000 cm^{-1}, similar to those reported by Rieley et al.[10] The IR bands are associated with the hydrated hydronium ion,[7] rather than with either the bulk amorphous monohydrate, which has an intense band near 2550 cm^{-1}, or molecular HCl, and cannot be assigned to any particular hydrate. We conclude that the surface species formed at temperatures between 85 and 125 K is a hydrated, partially ionized species, with a surface stoichiometry of HCl·H_2O. Below 125 K this species does not incorporate into the ice on the time scale of these experiments. We will refer to this surface-adsorbed HCl as the "surface monohydrate" on the basis of its stoichiometry to the surface water, although we cannot determine whether

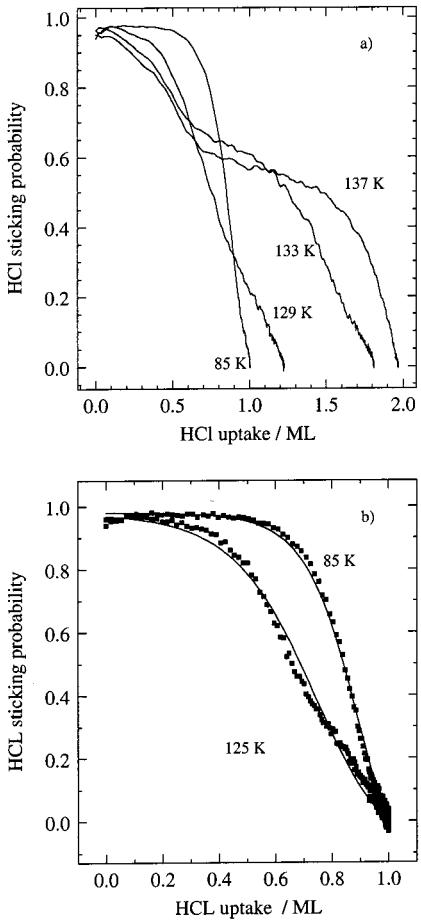

Figure 3. (a) Variation in $S(\Theta)$ with temperature for HCl adsorption onto 5.6 monolayers of crystalline ice. (b) Simulation of HCl adsorption on to the ice film at 85 and 125 K using the trapping model described in the text.

rearrangement of the next water bilayer occurs in order to further hydrate the adsorbed HCl.

C. HCl Adsorption on Crystalline Ice at 125 < *T* < 137 K. As the adsorption temperature is increased to 140 K, the initial HCl sticking probability at zero coverage (S_0) drops only slightly. This is shown in Figure 3a for a thin (5.6 monolayers) ice layer, S_0 remaining above 0.95 for all surface temperatures between 85 and 137 K. This behavior implies that the trapping probability and subsequent competition between desorption and hydration to form a stable species does not change significantly, the lifetime of the precursor toward desorption being sufficient to ensure that adsorption dominates over desorption. However, at higher temperatures the sticking probability begins to decrease before the HCl uptake reaches the 1 monolayer coverage achieved at low temperatures. Since trapping probabilities typically change only slowly with temperature and HCl scattering studies[22] have shown that the trapping probability on water ice surfaces remains large even at temperatures of 180 K, the decrease in sticking at higher surface temperatures can be attributed to a decrease in lifetime of the precursor on the HCl covered surface; HCl which has trapped desorbs before it is able to find a favorable hydration site on the ice surface.

On this basis the sticking probability can be described by a kinetic model which relates the relative rates of desorption and adsorption to form a stable hydrated species,

$$\mathrm{HCl(g)} \underset{k_d}{\overset{\alpha}{\rightleftarrows}} \mathrm{HCl(p)} \xrightarrow{k_a} \mathrm{HCl(a)}$$

where HCl(p) is the molecular precursor state and HCl(a) is the stable adsorbed state for HCl on the surface. This state saturates at $\Theta = 1$ monolayer with formation of a complete layer of HCl monohydrate. Assuming that the trapping probability, α, is approximately independent of temperature between 85 and 125 K allows us to estimate the difference between the rates for desorption and transfer into the chemisorbed state as a function of the HCl uptake onto the surface. Taking the rates of desorption and transfer into the adsorbed state as being first order, with rate constants k_d and k_a, the sticking probability is given by[44,45]

$$S(\Theta) = \alpha K(1 - \Theta)/\{1 + K(1 - \Theta)\}$$

where $K = k_a/k_d$ is the ratio of the rate constants for transfer to the chemisorbed state and desorption, respectively, and Θ is the HCl coverage in monolayers. The barrier to transfer out of the precursor state into the chemisorbed state may be expected to depend on the HCl coverage, reflecting changes to the stability of the final chemisorbed state as the surface coverage increases toward saturation at $\Theta = 1$ monolayer. This behavior is reflected in the decrease in sticking probability at higher temperatures for the HCl-covered surface. The solid curves in Figure 3b show the result of fitting the sticking behavior at $T \leq 125$ K and were obtained by making the (crude) assumption that the difference in activation barriers varies linearly with coverage, Θ. Taking a Polanyi−Wigner form for the rate constants k_d and k_a allows an estimate of $\Delta E_A = E_a - E_d = (-7.1 + 4.8\Theta)$ kJ mol^{-1} (where Θ is the HCl coverage in monolayers) for the difference in activation barriers to adsorption (E_a) and desorption (E_d) from the precursor state. As the HCl coverage increases the stability of the final hydrate is reduced, giving a concomitant increase in the barrier to chemisorption and a reduction in ΔE_A.

For ice films at 125 K or below the differences in $S(\Theta)$ are confined to a slight decrease in the sticking probability for $\Theta > 0.5$ monolayer but the saturation uptake of HCl remains $\Theta = 1$ monolayer within experimental error. However, although the decrease in sticking probability with HCl uptake persists above 125 K for $0 < \Theta < 1$ monolayer, uptake of HCl continues at higher exposures, Figure 3a. For temperatures between 127 and 133 K, HCl uptake does not cease abruptly at 1 monolayer, slow adsorption continuing with a sticking probability which is too low to be measured accurately by the direct reflection technique ($S < 10^{-2}$). At higher temperatures HCl adsorption remains efficient and shows a clear saturation behavior even for thick films of ice. This is shown in Figure 4 where efficient HCl adsorption at 136 K is contrasted with the slow uptake observed at 130 K. The final saturation uptake of HCl was determined by TPD and showed that above 125 K the saturation uptake of HCl slowly approaches that obtained during adsorption at $T \geq 134$ K. Above 140 K the HCl/ice films become unstable and HCl and H_2O desorb on the time scale of these experiments.

The increase in HCl uptake is associated with transport into the ice, as can be seen from the steady increase in HCl uptake as the thickness of the films is increased, Figure 5. By measuring the saturation uptake of HCl as a function of film thickness we can establish the stoichiometry of the bulk HCl hydrate product for thick ice films (>10 monolayers) to be HCl·(3.1 ± 0.3)-H_2O for adsorption at surface temperatures between 135 and 138 K. The stoichiometry of the HCl hydrate does not change for ice films 4 or more monolayers thick, Figure 5, although thick layers (40−150 monolayers of ice were used) require an extended exposure in order to saturate. The formation of HCl trihydrate in the temperature range 125−137 K is consistent with the phase diagram for HCl in ice[2] and with recent laser

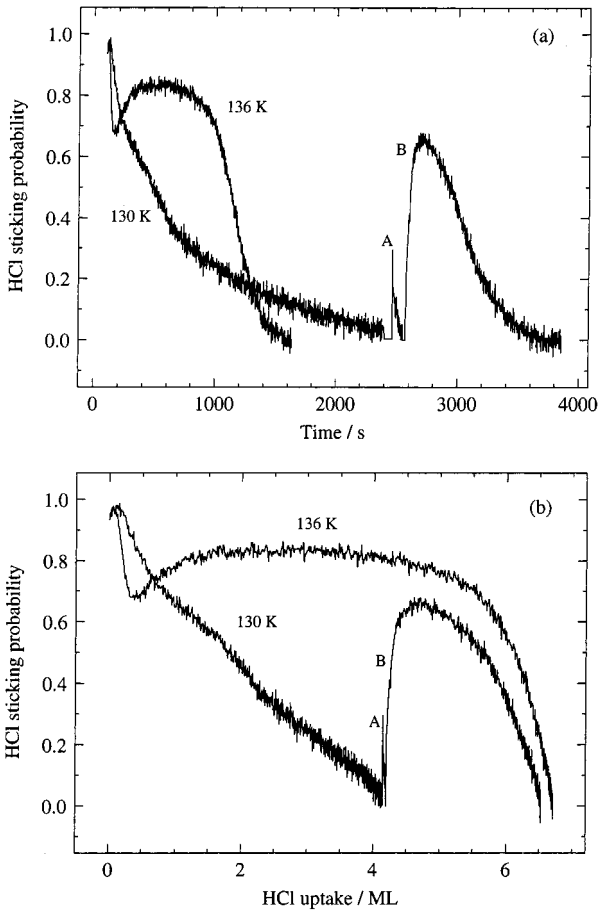

Figure 4. HCl adsorption onto a 20-monolayer film of crystalline ice at 136 and 130 K as a function of exposure time (a) and uptake (b). Adsorption at 136 K shows clear saturation behavior, whereas sticking continues slowly at 130 K. At 130 K interrupting the HCl beam briefly (A) results in a transient increase in *S*, while warming the surface to 136 K (B) results in increased HCl transport and rapid saturation of the film.

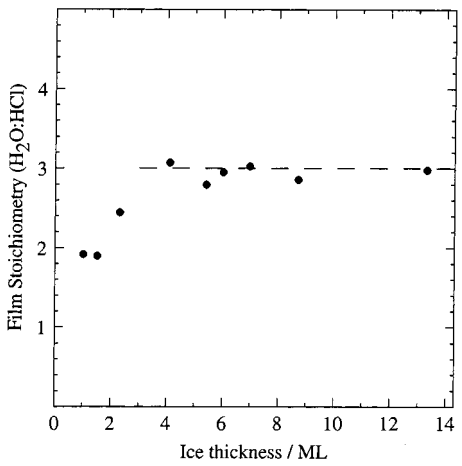

Figure 5. Stoichiometry of the hydrate produced by HCl saturation at 137 K as a function of the thickness of the ice film showing formation of HCl trihydrate for ice films thicker than ca. 4 monolayers.

induced thermal desorption measurements of the film composition.[23] We were unable to find any conditions under which the hexahydrate was stable, in good agreement with George and co-workers[23] who found a continuous change in stoichiometry above 148 K, with no evidence for formation of a specific hexahydrate phase. The RAIR spectra for HCl trihydrate formed from 70 ML of crystalline ice is shown in Figure 1a (iii) and

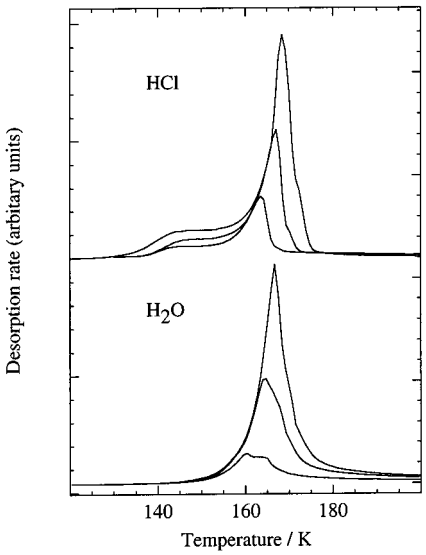

Figure 6. HCl and water desorption from 7, 11, and 20 bilayer thick ice films saturated with HCl at 137 K to form the trihydrate. The 20-monolayer film has been exposed to HCl as the surface is cooled to 85 K, resulting in an increased uptake of HCl onto the surface and a shift in the onset of HCl desorption down to 130 K.

shows bands at 1218, 1791, and 3397 cm^{-1}. These bands sharpen and shift slightly to 1231, 1741, and 3310 cm^{-1} as the film is heated above 170 K during desorption. The composition of this film (as determined by TPD) remains $HCl{\cdot}3H_2O$ and these changes appear to be associated with ordering to form a crystalline hydrate. The HCl trihydrate IR spectra (Figure 1iii,-iv) are very similar to those previously assigned to the hexahydrate,[7] which has been taken to be the saturation phase.[9] This assignment has been questioned by Banham et al.[11] in view of the absence of any evidence for a stable HCl tetrahydrate phase.

Figure 5 also shows that the metal support plays a role in determining the final $HCl:H_2O$ stoichiometry for the first few ice layers on the Pt(111) surface. For a single bilayer of ice the uptake of HCl at 137 K is 0.5 monolayer and the uptake increases to 1 monolayer for 2 bilayers of ice, before reducing to 1:3 for thicker ice layers. This is probably the result of an image charge interaction between the HCl hydrate and the metal substrate, which helps to stabilize charge separation in the partially ionized hydrate close to the Pt, as well as to direct binding of chloride on the surface.[46] Despite the change in product stoichiometry there is no noticeable change in the sticking probability for thin ice films, consistent with the conclusion that adsorption occurs via a precursor state followed by efficient adsorption to create the surface monohydrate.

When an ice film is saturated with HCl at 137 K to form HCl trihydrate, blocking the HCl beam from the surface results in a small amount of HCl desorption that ceases after a fraction of a monolayer of HCl has desorbed. Cooling the trihydrate film to 85 K and exposure to the HCl beam results in the uptake of less than 1 monolayer of HCl onto the surface. This adsorption−desorption cycle is reversible, HCl desorbs at around 130 K when the film is heated, whereas HCl from the bulk trihydrate film only starts to desorb above 140 K, Figure 6. The additional HCl uptake does not increase with film thickness and is associated with HCl adsorbed on the surface. The amount of HCl adsorbed is consistent with formation of a thin layer of higher stoichiometry on the surface of the trihydrate film, analogous to the "monohydrate" formed by adsorption on pure ice below 120 K (although the exact stoichiometry cannot be established, since the surface water density of the amorphous trihydrate film is not known). Temperature-programmed desorption measurements show that this additional HCl has an activation barrier to desorption of 31 kJ mol^{-1}, approximately half that of HCl desorbing from a bulk trihydrate film. It should be noted that the low-temperature tail to the HCl desorption trace (Figure 6), which develops into a separate feature for thicker ice films, is not due to a distinct HCl adsorption state but results from the kinetics of HCl desorption from these films.[47] Whereas this surface layer of HCl desorbs from the trihydrate film at 130 K, on pure ice transport into the film dominates over desorption and as a result the binding energy cannot be quantified.

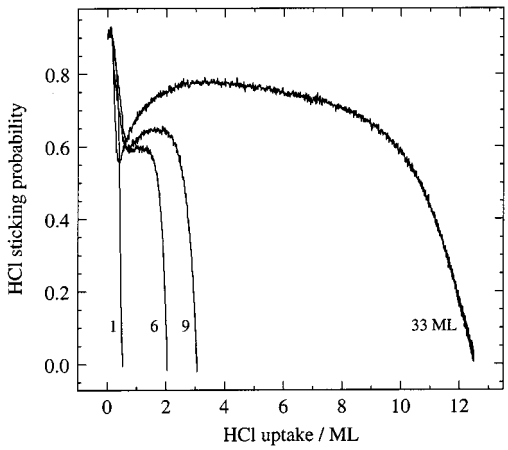

Figure 7. HCl adsorption on crystalline ice films at 137 K showing the development of a minimum in $S(\Theta)$ for thicker ice films. The ice thickness is 1, 6, 9, and 33 monolayers.

D. Incorporation of HCl into Ice Films at 137 K. Above 130 K HCl is incorporated into the ice films at a rate that is comparable to the dosing rate. Sticking shows a complicated kinetic behavior, Figures 3a and 4, depending on both the film thickness and the flux of HCl. At 137 K a minimum develops in the sticking probability as the film thickness is increased, Figure 7. At higher exposures the adsorption probability increases again and reaches a maximum after several monolayers of HCl has been adsorbed. After this the sticking probability decreases only very slowly as HCl is adsorbed, before falling as the film becomes saturated with HCl. The development of a distinct minimum in $S(\Theta)$ at an HCl uptake below 1 monolayer requires an ice film at least 5 monolayers thick and the value of S, and the HCl coverage for which this occurs, is sensitive to the flux of HCl and to the preparation of the ice film. The minimum in $S(\Theta)$ is most pronounced for thick ($\geq$10 monolayers), highly crystalline ice films where it occurs for an uptake near 0.5 monolayers, Figure 7. Increasing the flux of HCl increases the amount of HCl adsorbed before S reaches a minimum, Figure 8, but this uptake is always less than 1 monolayer. Changing the flux of the HCl beam also changes the degree to which the adsorption probability recovers after the initial uptake of HCl. Low fluxes of HCl result in a large sticking probability, whereas high fluxes suppress the recovery in S at longer times, Figure 8.

The uptake behavior on ASW, Figure 9, is broadly similar to that on crystalline ice and the saturation composition of films more than a few bilayers thick is $HCl{\cdot}3H_2O$, identical to that for crystalline ice. A minimum forms in $S(\Theta)$ near 1 monolayer uptake of HCl, followed by a small recovery in the sticking probability as adsorption proceeds. However, there are several quantitative differences in the HCl uptake compared to that on crystalline ice Ih. First, the minimum in the HCl sticking is not

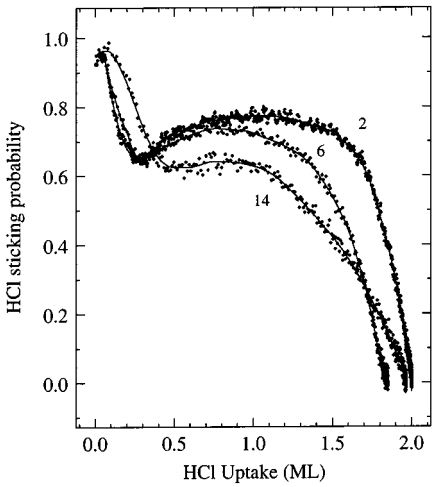

Figure 8. Flux dependence of HCl adsorption onto a 5-monolayer thick ice film showing the decrease in S for increasing flux. The HCl flux was 2, 6, and 14 x 10^{-3} monolayer s^{-1}.

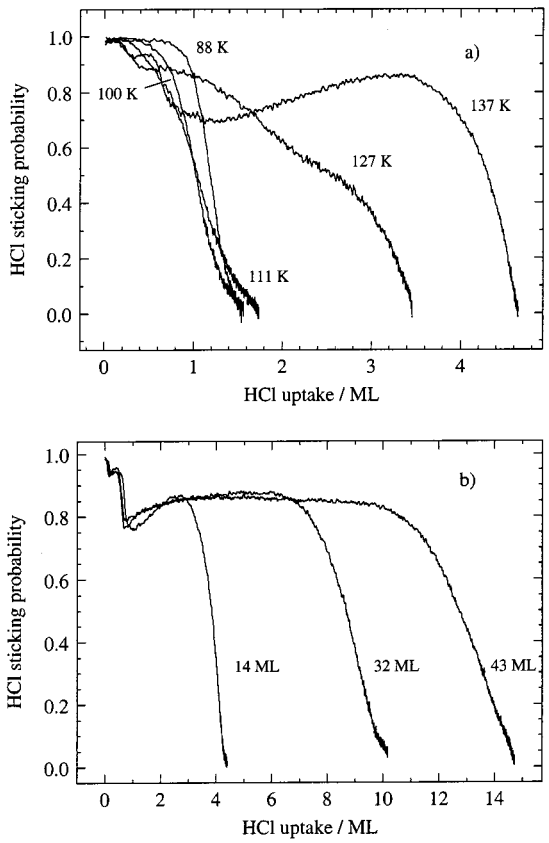

Figure 9. HCl adsorption on ASW (a) as a function of temperature on a 14-monolayer thick film and (b) as a function of film thickness at 137 K.

so pronounced as for crystalline ice, Figure 7, and once the sticking probability has recovered, $S(\Theta)$ remains almost constant until the film begins to saturate, whereas a slow but steady drop in $S(\Theta)$ is seen during adsorption on the ice Ih film. Second, a clear step is seen in the adsorption behavior in the submonolayer coverage regime, Figure 9a, $S(\Theta)$, before the minimum is reached. The presence of this step is quite repeatable, and insensitive to the substrate used or precise details of how the ASW film is grown. It is probably associated with rapid saturation of HCl uptake on regions of the rough ASW surface from which the precursor state cannot migrate to favorable adsorption sites. Annealing the ASW ice reduces the surface area of the films and removes this structure, but only when the ice film begins to show the sharp RAIRS structure associated with crystalline ice.

The minimum in $S(\Theta)$ appears to be associated with the uptake of HCl onto the surface to form a layer of HCl hydrate on the surface, prior to the onset of HCl incorporation into the ice film. Increasing the flux of HCl increases the amount of HCl adsorbed before S reaches a minimum, Figure 8, but this uptake is always less than 1 monolayer. This behavior is consistent with a transient equilibrium being established between adsorption to form a partially saturated monohydrate surface and desorption back to the gas phase. We have seen that a fraction of a monolayer of HCl adsorbs on the HCl trihydrate surface at $T < 125$ K and desorbs again above 130 K, Figure 6. If we assume that the clean ice surface during adsorption has similar adsorption sites to the HCl trihydrate surface, then increasing the HCl flux will increase the amount of gas adsorbed on the surface before the equilibrium with HCl desorption is established, leading to a minimum in $S(\Theta)$ which increases with flux. More direct evidence for the change in the equilibrium surface coverage on the ice film is masked by the onset of incorporation into the bulk.

Changing the flux of the HCl beam also changes the degree to which the adsorption probability recovers after the initial uptake of HCl. Low fluxes of HCl result in a large sticking probability, whereas high fluxes suppress the recovery in S at longer times, Figure 8. This can be explained if HCl adsorption is kinetically limited by the formation of free adsorption sites on the surface as HCl is transported into the bulk of the ice film. Increasing the HCl flux ensures that surface sites on which HCl could adsorb are refilled faster than HCl can transport away from the surface. As a result HCl molecules find a fully saturated HCl hydrate surface and the sticking probability drops. Conversely, reducing the flux of gas gives HCl time to transport away from the surface, reducing the equilibrium coverage of surface adsorbed HCl and so increasing the density of vacant adsorption sites and the sticking probability. Interrupting the HCl flux has a similar effect, (see A in Figure 4), allowing HCl to transport away from the surface while the beam is blocked and expose fresh sites for adsorption. When the HCl beam is readmitted the sticking probability has increased but falls rapidly as the vacant sites are filled. In contrast, increasing the temperature permanently increases the HCl transport rate into the film and the uptake increases until the film is saturated (B in Figure 4). Even at these low temperatures, where water desorption is negligible, HCl can transport hundreds of monolayers into a crystalline ice film, with an adsorption rate of at least 10^{-2} monolayer s^{-1} at 137 K.

Once the initial drop and recovery has been completed, thick ice Ih films at 137 K show a slow but steady decrease in sticking probability until the film begins to saturate with HCl, Figure 7. For a flux of 0.015 monolayer s^{-1} at 137 K this fall-off in S occurs with a range on the order of 100 monolayers of HCl adsorbed. Under the same conditions the sticking probability on ASW is independent of uptake and HCl flux, Figure 9, consistent with adsorption being limited by the HCl flux rather than by transport into the ASW film. This implies that HCl transport into the ASW film is fast compared to that into the crystalline ice film. At low HCl fluxes, where there is time for HCl to transport away from the surface, the sticking probability does not increase above ~0.8 on either surface, indicating that absorption is probably limited by HCl trapping−adsorption at the surface rather than by transport into the film. Only when the HCl flux is increased above ca. 10^{-2} monolayer s^{-1} during

adsorption on ice Ih (Figure 8) is there a decrease in the uptake probability, indicating that surface sites are becoming blocked and HCl transport is becoming rate limiting.

The recovery in the HCl sticking probability after its initial drop is unexpected and indicates that the availability of favorable HCl adsorption sites increases as HCl starts to transport into the ice film. We can propose two possible reasons for this, either the effective surface area of the films increases as HCl trihydrate is formed or the rate of HCl transport into the ice surface increases as HCl is incorporated into the surface. The first explanation does not seem to be consistent with the data, since the increased HCl adsorption rate is maintained until the film saturates with HCl. If the surface area alone increased during HCl adsorption, this would give a brief increase in the HCl adsorption rate, associated with filling the new surface sites, whereas we find that the rate of HCl transport into the ice has increased permanently as HCl begins to incorporate into the film. We believe that the increase in the HCl transport rate is associated with disruption of the crystalline structure of the ice as HCl is incorporated into the film. Livingston and George have reported an increase in the diffusion coefficient for HDO into an ice film which has been doped with HCl,[48] the rate of diffusion increasing by a factor of 10−20 compared to that on pure ice. This behavior was insensitive to the amount of HCl dosed, suggesting that incorporation of HCl disrupts the hydrogen-bonding network in the ice lattice and enhances both the diffusion rate and the rate of water desorption.[49] Since the HCl hydrate diffusion rate at higher temperatures is similar to that for water, diffusion of both species probably occurs by creating vacant defect sites in the lattice.[50] The increased HCl transport rate into ASW films compared to crystalline ice Ih is consistent with this picture, the higher defect density in ASW leading to a higher transport rate. Similarly, a reduction in the contrast of the initial dip in $S(\Theta)$ indicates that the presence of HCl in the ASW film makes a smaller difference in the transport rate. This is consistent with HCl incorporation making less difference to the defect density of the disordered ASW film, reducing the influence of HCl in promoting transport into the film.

4. Discussion

Exposing a crystalline ice Ih surface to HCl at temperatures below 125 K results in the adsorption of one HCl for each water molecule in the surface bilayer, to give a coverage of 1.1 x 10^{15} molecules cm^{-2}. The absence of IR bands due to molecular HCl and the presence of broad weak bands associated with the hydroxonium species indicate that this species is dissociated, in agreement with previous conclusions. The adsorption behavior is consistent with HCl trapping into a molecular precursor state which is mobile on the surface, before finding a favorable site for dissociation. The HCl sticking probability remains identical on a disordered ASW surface, an increased uptake probably reflecting the larger surface area of the film. Whereas several calculations have suggested that the barrier to HCl ionization is too large for surface adsorbed HCl to dissociate,[16,28] a recent model of adsorption onto the ice Ih surface found that a molecule trapped on the surface could dissociate when it encountered a favorable site.[19] Ionization was nonactivated when HCl adsorbed at a water site where one of the molecules in the upper half of the water bilayer has a free (non-hydrogen-bonded) O atom and the other two adjacent molecules have dangling H atoms. The chloride ion formed was stable, sitting at the center of a distorted water hexagon,[20] and on this basis a maximum surface coverage of $^1/_3$ monolayer of HCl was predicted.[19] This is clearly inconsistent with adsorption of 1 monolayer of HCl during saturation at $T \leq 125$ K and we could see no evidence for formation of a distinct submonolayer phase, although adsorption does become less favorable as the HCl coverage increases. However, the predicted saturation coverage is based on the assumption that the chloride remains adsorbed on the surface and the simulations did show a tendency for it to penetrate below the surface water, suggesting that hydration into the surface may occur rapidly compared to experimental time scales, therefore freeing up sites for further adsorption.

Only above 125 K is transport into the bulk observed as HCl hydrates further and is incorporated into the ice film. Above 135 K HCl adsorption saturates with formation of a trihydrate film ($HCl{\cdot}3H_2O$), irrespective of the original ice morphology and with no evidence for the intermediate formation of any other hydrate phases. This is in agreement with a recent laser-induced desorption study of the saturation composition under similar conditions which found the trihydate below 148 K followed by a steady decrease in the HCl concentration at higher temperatures.[23] The IR spectrum of the amorphous trihydrate film is similar to that ascribed to the hexahydrate in the literature.[11] At low temperatures, further HCl will adsorb on the trihydrate to form an HCl rich surface, probably analogous to the surface hydrate formed on ice at $T < 125$ K, the additional HCl desorbing when the film is heated to 130 K.

As the temperature is increased the initial sticking probability remains constant, but as the coverage gets higher desorption from the precursor state starts to compete effectively with HCl adsorption into the stable surface species. On a clean ice surface ($\Theta = 0$) Isakson and Sitz[21] found activation barriers of 28 and 21 kJ mol^{-1} for HCl desorption and loss processes during scattering, in good agreement with the difference of 7 ± 1.5 kJ mol^{-1} found here for the bare ice surface. This is consistent with the loss process they observed, which is hydration of HCl to form the stable surface-adsorbed species. We cannot determine the binding energy of the surface HCl hydrate formed since HCl simply incorporates into the ice film on heating; however, the activation barrier to desorption from the trapping state (28 kJ mol^{-1} [21]) is similar to that found for HCl adsorbed on the surface of the trihydrate film (31 kJ mol^{-1}).

The increase in transport rate as HCl starts to incorporate into the ice lattice seen at 137 K (Figure 7) is consistent with the formation of a metastable hydrate layer on the surface, HCl initially incorporating into the surface slowly before absorption disrupts the ice lattice and the rate of HCl transport accelerates. This is consistent with recent measurements of water and HCl hydrate diffusion by Livingston and George[48,50] who reported an increase in the diffusion rates in ice film which has been doped with HCl.[48] This behavior was attributed to HCl disrupting the hydrogen bonding network, creating vacant defect sites in the lattice which enhance the diffusion rate. During HCl absorption into the film we do not see any evidence for a change in the HCl incorporation rate which might be attributed to the formation of a stoichiometric phase, e.g. the hexahydrate, before adsorption saturates with formation of an HCl trihydrate film.

HCl adsorption at high fluxes, as the film approaches saturation, Figures 7 and 9, and at lower temperatures, Figure 4, is limited by transport of HCl away from the surface (or water to the surface) to create vacant sites for further HCl adsorption. It is not clear that transport of HCl away from the surface during adsorption from the gas phase can be described properly by a diffusion model. HCl adsorption and transport into the film is irreversible, driven by exothermic hydration to form the stable trihydrate. Nevertheless, diffusion models have been applied

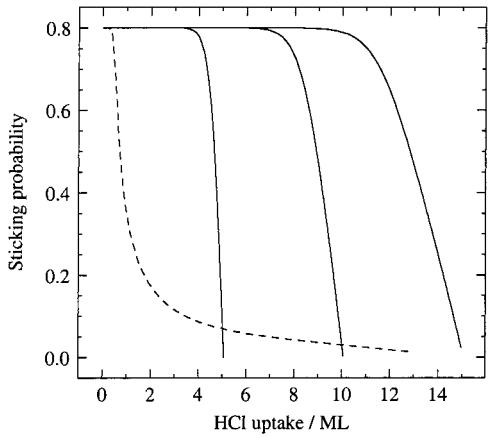

Figure 10. Adsorption of HCl onto ice films of different thickness with $D = 5 \times 10^{-15}$ cm^2 s^{-1}. $S(\Theta)$ is assumed to be given by a smooth function (solid lines, see text) and the dotted curve shows the effect of reducing the diffusion coefficient to 1×10^{-16} cm^2 s^{-1} for a 45-monolayer thick ice film.

to HCl transport in ice films even when large concentration gradients are present. Measurements of the temperature dependence for HCl trihydrate diffusion into an ice layer above 170 K indicate that the diffusion rate was independent of the HCl concentration[50] and significantly larger than the diffusion rate for dilute HCl solutions. These data can be extrapolated to give an estimate of $D \sim 6 \times 10^{-18}$ cm^2 s^{-1} at 137 K,[50] comparable to the coefficient for water diffusion into an HCl doped ice film, $D = 1.2 \times 10^{-18}$ cm^2 s^{-1} at 137 K.[48] Since HCl sticking depends on the formation of a vacant surface site, it is interesting to see if diffusion of HCl trihydrate into the ice film can provide an adequate model for HCl adsorption on thick films and compare the transport rate with that predicted.

Adsorption at 137 K can be simulated by assuming that the sticking probability depends on the surface coverage, with new adsorption sites being formed as HCl diffuses into the bulk. This requires some assumption about the form of $S(\Theta)$, since this cannot be determined independently at this temperature. HCl is assumed to trap onto the surface with a probability $\alpha \sim 0.8$ and a sticking probability $S(\Theta)$ which remains constant until the surface is nearly saturated. Adsorption is calculated assuming either that S remains constant until $\Theta = \Theta_{sat}$ or, more realistically, that S starts to drop somewhat before saturation (see Figure 2, for example). This is illustrated by taking $S(\Theta) = \alpha(1 - (\Theta/\Theta_{sat})^{20})$, solid lines Figure 10, and the uncertainty in the form of S near saturation prevents us from obtaining more than a lower limit for the diffusion coefficient D. The diffusion model provides a reasonable description of adsorption on the ASW ice surface, reproducing the change in slope of $S(\Theta)$ as saturation approaches over a wide range of film thickness. The model cannot reproduce the change in S with flux on the crystalline ice surface without additional information describing the HCl desorption rate from the ice surface. If we use the diffusion values estimated from Livingston and George, $D = (1-6) \times 10^{-18}$ cm^2 s^{-1}, we find that transport into the ice film should be negligible, the surface rapidly forming a film of HCl trihydrate and adsorption ceasing, Figure 10. Only by using diffusion coefficients some 3 orders of magnitude larger ($D \sim (3-5) \times 10^{-15}$ cm^2 s^{-1}) could we reproduce incorporation of HCl into the ice film on the observed time scale.

Horn and Sully[51] also measured diffusion coefficients some 4 orders of magnitude greater than the LITD estimates at 150 K by following HCl incorporation into thin films using FTIR. It was suggested that that increased diffusion rates might be due to defects in the ice films,[50] but the high transport rates observed here occur even on highly ordered films and support a much greater transport rate than suggested by the LITD diffusion measurements. It seems likely that the discrepancy between the adsorption and diffusion measurements originates in the different HCl concentrations in the two experiments. During the LITD experiments the degree of hydration of HCl probably changes relatively little as HCl diffuses into the surrounding ice. However, during adsorption HCl uptake is driven by hydration which is exothermic. This leads to a surface film forming which has an excess of HCl and incomplete hydration. HCl adsorption and growth of the trihydrate film in these experiments is associated with rapid irreversible transport within the HCl hydrate layer driven by hydration of the excess HCl. Depending on the relative transport rates in the hydrate and ice films, this may form a well-defined reaction boundary to the ice underneath, in which HCl transport is slower.

5. Conclusions

HCl adsorption on water ice below 120 K forms a surface layer of an HCl hydrate with a saturation uptake of one HCl for each water molecule in the surface bilayer. Adsorption is efficient and the initial sticking probability is insensitive to the morphology of the film, occurring via a precursor state. The resulting film shows broad IR bands characteristic of H_3O^+, indicating significant ionization of the HCl. Above 125 K, HCl starts to transport into the ice, forming HCl trihydrate. This film has an IR spectrum similar to that previously ascribed to the hexahydrate. Further adsorption of a submonolayer film of HCl on the trihydrate surface is reversible, desorption occurring around 130 K with an activation barrier of 31 kJ mol^{-1}. HCl transport into the ice is irreversible and is driven by HCl hydration, the rate accelerating as HCl disrupts the ice lattice. In this regime the adsorption probability is flux dependent, HCl adsorption being limited by the production of stable binding sites on the ice surface as HCl transports into the bulk with a first-order rate in excess of 10^{-2} monolayer s^{-1} at 137 K.

Acknowledgment. We acknowledge NERC support of this work.

References and Notes

(1) Hanson, D.; Mauersberger, K. *Geophys. Res. Lett.* **1988**, *15*, 1507.
(2) Hanson, D. R.; Mauersberger, K. *J. Phys. Chem.* **1990**, *94*, 4700.
(3) Abbatt, J. P. D.; Beyer, K. D.; Fucaloro, A. F.; McMahon, J. R.; Wooldridge, P. J.; Zhang, R.; Molina, M. J. *J. Geophys. Res. Atmos.* **1992**, *97*, 15819.
(4) Lee, S. H.; Leard, D. C.; Zhang, R. Y.; Molina, L. T.; Molina, M. J. *Chem. Phys. Lett.* **1999**, *315*, 7.
(5) Barone, S. B.; Zondlo, M. A.; Tolbert, M. A. *J. Phys. Chem. A* **1999**, *103*, 9717.
(6) Ritzhaupt, G.; Devlin, J. P. *J. Phys. Chem.* **1991**, *95*, 90.
(7) Delzeit, L.; Rowland, B.; Devlin, J. P. *J. Phys. Chem.* **1993**, *97*, 10312.
(8) Graham, J. D.; Roberts, J. T. *J. Phys. Chem.* **1994**, *98*, 5974.
(9) Graham, J. D.; Roberts, J. T. *Geophys. Res. Lett.* **1995**, *22*, 251.
(10) Rieley, H.; Aslin, H. D.; Haq, S. *J. Chem. Soc., Faraday Trans.* **1995**, *91*, 2349.
(11) Banham, S. F.; Sodeau, J. R.; Horn, A. B.; McCoustra, M. R. S.; Chesters, M. A. *J. Vac. Sci. Technol. A* **1996**, *14*, 1620.
(12) Banham, S. F.; Horn, A. B.; Koch, T. G.; Sodeau, J. R. *Faraday Discuss.* **1995**, 321.
(13) Uras, N.; Rahman, M.; Devlin, J. P. *J. Phys. Chem. B* **1998**, *102*, 9375.
(14) Kroes, G. J.; Clary, D. C. *J. Phys. Chem.* **1992**, *96*, 7079.
(15) Wang, L. C.; Clary, D. C. *J. Chem. Phys.* **1996**, *104*, 5663.
(16) Gertner, B. J.; Hynes, J. T. *Science* **1996**, *271*, 1563.
(17) Bussolin, G.; Casassa, S.; Pisani, C.; Ugliengo, P. *J. Chem. Phys.* **1998**, *108*, 9516.
(18) Casassa, S. *Chem. Phys. Lett.* **2000**, *321*, 1.

(19) Svanberg, M.; Pettersson, J. B. C.; Bolton, K. *J. Phys. Chem. A* **2000**, *104*, 5787.
(20) Bolton, K.; Pettersson, J. B. C. *J. Am. Chem. Soc.* **2001**, *123*, 7360.
(21) Isakson, M. J.; Sitz, G. O. *J. Phys. Chem. A* **1999**, *103*, 2044.
(22) Andersson, P. U.; Nagard, M. B.; Pettersson, J. B. C. *J. Phys. Chem. B* **2000,** *104*, 1596.
(23) Foster, K. L.; Tolbert, M. A.; George, S. M. *J. Phys. Chem. A* **1997**, *101*, 4979.
(24) Sadtchenko, V.; Giese, C. F.; Gentry, W. R. *J. Phys. Chem. B* **2000**, *104*, 9421.
(25) Kroes, G. J.; Clary, D. C. *Geophys. Res. Lett.* **1992**, *19*, 1355.
(26) Robertson, S. H.; Clary, D. C. *Faraday Discuss.* **1995**, 309.
(27) Clary, D. C.; Wang, L. C. *J. Chem. Soc., Faraday Trans.* **1997**, *93*, 2763.
(28) Bianco, R.; Gertner, B. J.; Hynes, J. T. *Ber. Bun. Phys. Chem.* **1998**, *102*, 518.
(29) Starke, U.; Heinz, K.; Materer, N.; Wander, A.; Michl, M.; Doll, R.; van Hove, M. A.; Somorjai, G. A. *J. Vac. Sci. Technol. A* **1992**, *10*, 2521.
(30) Ogasawara, H.; Yoshinobu, J.; Kawai, M. *J. Chem. Phys.* **1999**, *111*, 7003.
(31) Ogasawara, H.; Yoshinobu, J.; Kawai, M. *Chem. Phys. Lett.* **1994**, *231*, 188.
(32) Morgenstern, M.; Muller, J.; Michely, T.; Comsa, G. *Z. Phys. Chem.* **1997**, *198*, 43.
(33) Glebov, A.; Graham, A. P.; Menzel, A.; Toennies, J. P. *J. Chem. Phys.* **1997**, *106*, 9382.
(34) Materer, N.; Starke, U.; Barbieri, A.; VanHove, M. A.; Somorjai, G. A.; Kroes, G. J.; Minot, C. *Surf. Sci.* **1997**, *381*, 190.
(35) Smith, R. S.; Kay, B. D. *Nature* **1999**, *398*, 788.
(36) Stevenson, K. P.; Kimmel, G. A.; Dohnalek, Z.; Smith, R. S.; Kay, B. D. *Science* **1999**, *283*, 1505.
(37) Materer, N.; Starke, U.; Barbieri, A.; Vanhove, M. A.; Somorjai, G. A.; Kroes, G. J.; Minot, C. *J. Phys. Chem.* **1995**, *99*, 6267.
(38) Glebov, A.; Graham, A. P.; Menzel, A.; Toennies, J. P.; Senet, P. *J. Chem. Phys.* **2000**, *112*, 11011.
(39) Harnett, J.; Haq, S.; Hodgson, A. *Surf. Sci.*, in press.
(40) King, D. A.; Wells, M. G. *Surf. Sci.* **1972**, *29*, 454−482.
(41) Morgenstern, M.; Michely, T.; Comsa, G. *Phys. Rev. Lett.* **1996**, *77*, 703.
(42) Callen, B. W.; Griffiths, K.; Norton, P. R. *Surf. Sci.* **1992**, *261*, L44.
(43) Dohnalek, Z.; Ciolli, R. L.; Kimmel, G. A.; Stevenson, K. P.; Smith, R. S.; Kay, B. D. *J. Chem. Phys.* **1999**, *110*, 5489.
(44) Kisliuk, P. J. *J. Phys. Chem. Solids* **1958**, *5*, 78.
(45) Cassuto, A.; King, D. A. *Surf. Sci.* **1981**, *102*, 388.
(46) Nakamura, M.; Song, M. B.; Ito, M. *Chem. Phys. Lett.* **2000**, *320*, 381.
(47) Harnett, J.; Haq, S.; Hodgson, A. In preparation.
(48) Livingston, F. E.; George, S. M. *J. Phys. Chem. B* **1999**, *103*, 4366.
(49) Livingston, F. E.; George, S. M. *J. Phys. Chem. A* **1998**, *102*, 10280.
(50) Livingston, F. E.; George, S. M. *J. Phys. Chem. A* **2001**, *105*, 5155.
(51) Horn, A. B.; Sully, J. *J. Chem. Soc., Faraday Trans.* **1997**, *93*, 2741.